Dynamics of the Inner Neptunian System: Proteus and Larissa

Ke Zhang and Douglas P. Hamilton

ABSTRACT

WARNING: This paper is still in production. Expect typos, small errors and missed references. A real abstract will appear here when we finish.

1. Introduction

Prior to Voyager 2 encounter, Neptune has two known satellites: large icy Triton and distant irregular Nereid. Triton is located where one usually finds regular satellites (close satellites in circular equatorial orbits, which have the same origin as their parent planets) around other planets, and moves nearly in a circle, but its orbit is retrograde and significantly tilted, which is common only among irregular satellites (small distant satellites in tilted and elongated orbits, which are thought to be captured minor planets). Triton's unique orbital properties imply a capture origin followed by an orbital evolution history featuring tidal damping and circularization (McKinnon 1984; Goldreich et al. 1989; Agnor and Hamilton 2005). Although different capture mechanisms have been proposed, Triton's post-captured orbit is remote and extremely eccentric in all scenarios. During its post-captured orbital circularization, Triton forced any of Neptune's original regular satellites into collision and self-disruption, and a debris disk formed. Most of the debris was ejected out of the system, or crashed onto Neptune or Triton, while some materials close to Neptune survived (Hamilton et al. 2005) to form a new generation of satellites. Banfield and Murray (1992) estimated the reforming timescale, which was in the order of tens of years. However, those survivors were unknown until the fly-by of Voyager 2 in 1989 (Smith et al. 1989).

Voyager 2 discovered six small satellites and several rings, and confirmed the ring arcs seen by occultation years earlier, all of which are closely around Neptune (within five Neptune radii). Karkoschka (2003) reexamined the Voyager 2 images later, and derived more accurate sizes and shapes of the new satellites. Proteus, the largest one, is only about 400 kilometers in diameter, which is smaller than even the smallest regular satellite of Uranus, Miranda. Owen et al. (1991) calculated their orbital elements, and Jacobson and Owen (2004) provided more precise measurements based on the data from Voyager 2, Hubble Space Telescope and ground-based observations. Both of these analyzes show that all the small moons are in direct near-circular orbits with moderate inclinations. Their parameters are listed in Table 1.

The short satellite formation timescale in the debris disk implies that satellites can form around the end of Triton's migration and circularization. However, Smith et al. (1989) calculated the cometary bombardment rate in that region and pointed out that only the outermost Proteus is able to survive disruptive collisions over the age of the Solar System. The innermost Naiad

probably could not last much longer than 2 to 2.5 billion years. For those four satellites between them, calculations based on the current small body flux show that they have reasonable surviving probabilities, but they would be destroyed during an early period of heavy bombardment. Hence it is very likely that all the six small satellites formed with the massive Triton in or close to its current tilted retrograde orbit. In this unique situation, the orbits of the small satellites might evolve differently from other moon systems. Reconstructing their orbital evolution history will enable us to place constraints on the tidal dissipation factor Q (see Goldreich and Soter 1966) of both Neptune and its satellites. Furthermore, the initial formation location of Proteus can constrain parameters of Triton's post-captured orbit.

The current inclinations of the six small satellites, albeit small, are clearly non-zero (Table 1). However, the debris disk, in which they formed, damps very quickly into a thin plane similar to Saturn's rings. For satellites formed out of this thin disk, their inclinations should be less than 0.001°. The observed values are much larger and imply that something excited these inclinations in the past. In this paper, we investigate the possibility of the resonance passage as an excitation mechanism. The satellites migrate (i.e., their semimajor axes change) due to tides, and pass through orbital resonances configurations, which kicks their inclinations up sharply. The same procedure can also explain the eccentricities of Larissa and Proteus, which, unlike other satellites, are significantly greater than zero. We provide some background information on the theory of tidal evolution and resonance passage in the next two sections. In section 5 we present our numerical results for different mean motion resonances between the two outermost small satellites and immediate implications. In the last section, we discuss our constraints on Triton's capture and Neptune's Q.

2. Tidal Evolution

Tidal friction between satellites and their mother planet determines their orbital evolution over a long time span (Darwin 1880; Burns 1977). The physical way in which tides affect orbits can be found in (Goldreich and Soter 1966; Burns 1977; Murray and Dermott 1999). The small satellites raise tides on Neptune (planetary tides), which then drive them to migrate either inwards or outwards, depending on their mean motion. If a satellite orbits faster than the rotation of Neptune, it moves towards the planet, or its semimajor axis decreases over time; otherwise, it moves away from the planet, and its orbit enlarges. The distance, at which a satellite's orbital period is the same as the spin period of its planet, is usually referred as synchronous radius (R_{syn}). The orbit at that distance is called synchronous orbit or co-rotation orbit. A satellite at synchronous orbit always faces the same side of its planet, and aligns with the tidal bulge it raises on the planet. For a satellite reasonably away from the synchronous orbit, its migration rate due to planetary tides is (Murray and Dermott 1999):

$$\frac{\dot{a}}{a} = \pm \frac{3k_{2N}}{Q_N} \frac{m}{m_N} \left(\frac{R_N}{a}\right)^5 n. \tag{1}$$

Here m, a, and n are the mass, semimajor axis. and mean motion of the satellite, respectively. m_N is Neptune's mass. The Love number k_{2N} measures the internal rigidity of Neptune. Q_N is the tidal dissipation factor of Neptune, which parametrizes the energy dissipation rate. Q_N generally depends on the amplitude and frequency of tides (Goldreich and Soter 1966), but this dependence is very weak for low frequency tides with small amplitudes. In this paper we assume constant Q's for both Neptune and its satellites. The plus sign in the above equation is for satellites inside R_{syn}, and minus sign is for those outside R_{syn}.

For the Neptunian system, the synchronous orbit lies between Larissa and Proteus (c.f. Fig. 1), which means Proteus's orbit has expanded while orbits of all other satellites have shrunk. The big gap between the orbits of Proteus and Larissa provides an evidence for the different migration directions. The migration time scales for those satellites are difficult to estimate because the uncertainty of Q_N (Goldreich and Soter 1966). Banfield and Murray (1992) estimated Q_N to be between 12,000 and 330,000. Based on this rough estimation, we found that the semimajor axes of those small satellites had changed in the order of R_N over the age of the Solar System. Although Triton is outside the synchronous orbit, it always moves towards Neptune due to its retrograde orbit. Being much further away from Neptune, it migrates a lot slower than the small satellites, with a timescale $\sim 10^{12}$ years. We can safely ignore its migration.

Tides not only change the size of an orbit, but also affect other orbital elements. Jeffreys (1961) showed that the eccentricity usually grows thanks to planetary tides. However, in the Neptunian system and most other moon systems, tides on a satellite raised by its planet damp the satellite's eccentricity and circularize its orbit. This damping effect dominates the eccentricity growth due to planetary tides (Goldreich 1963). The eccentricity damping rate can be found in Murray and Dermott (1999):

$$\frac{\dot{e}}{e} = -\frac{63}{4}\frac{1}{\tilde{\mu}Q}\frac{m_N}{m}\left(\frac{R}{a}\right)^5 n. \tag{2}$$

Here R is the radius of the satellite, Q is the tidal quality factor of the satellite, and $\tilde{\mu}$ is the ratio between the elastic to gravitational forces in the satellite tides – another measurement of internal strength.

Based on reasonable assumptions for Q_T and $\tilde{\mu}_T$, Goldreich and Soter (1966) estimated the circularization timescale for Triton, which is in the order of 100 million years. This is much shorter than the age of the Solar System, which means Triton has been tidally circularized in the very beginning and spend the majority of its time in current circular orbit. The eccentricity damping timescales for the small satellites is longer because their small sizes, but they are still much less than 1 billion years. The eccentricities of the four inner small moons are all consistent with zero. However, the orbits of Larissa and Proteus are considerably eccentric, which indicates a very recent excitation.

The inclination also changes due to tides because rotation carries the tidal bulge in and out of

orbital plane, but for a satellite with small tilt, the change rate is very slow (Burns 1977):

$$\frac{\dot{i}}{i} \approx -\frac{1}{4}\frac{\dot{a}}{a}. \tag{3}$$

For the inner Neptunian satellites, their inclinations only increase or decrease by less than a tenth of their values over the age of the Solar System. This means that any excitation of their orbital tilts in the past is permanent. Their current inclinations carry fossil evidences of their orbital evolution history.

3. Mean Motion Resonance Passage

A resonance happens when the frequency of a driven force matches the periodic behavior of a dynamical system. When the orbits of two satellites are perturbed by their mutual gravity, an orbit-orbit resonance, also known as a mean-motion resonance, occurs when commensurability exists between the two satellites, or the ratio between the periods of the satellites is a rational number. During a mean-motion resonance, the same orbital configuration repeats periodically, which means the orbits are continuously perturbed in the same way, resulting in dramatic changes of the orbital elements in a relatively short time. The resonance timescale is still much longer than the orbital period, but a lot shorter than the secular perturbation timescale. Physical representation of mean motion resonances can be found in Greenberg et al. (1972); Peale (1976); Greenberg (1977); Peale (1986).

If the orbit does not precess, resonances occur when the two orbits are exactly commensurate, and the satellite's eccentricity and inclination are excited at the same moment. In reality, however, both the oblateness of Neptune and secular perturbations from other satellites cause the orbit to process, leading to resonance splitting similar to the Zeeman effect in which an atomic line splits when the magnetic field is available. Instead of all the affected eccentricities and inclinations are kicked up simultaneously, they change at different time. The degenerated mean-motion resonance is replaced by a series of eccentricity-type, inclination-type, and combined-type resonances, depending on which orbital elements they affect.

An angular parameter is associated with any single resonance, known as resonant angle or resonant argument, which is in the form:

$$\phi = (p+q)\,\lambda_2 - p\,\lambda_1 + j_1\,\Omega_1 + j_2\,\Omega_2 + j_3\,\varpi_1 + j_4\,\varpi_2. \tag{4}$$

Here λ_1, Ω_1, ϖ_1 and n_2, Ω_2, ϖ_2 are the orbital mean longitudes, longitudes of ascending nodes, and longitudes of pericenters of the two satellites, respectively. The are two constraints for any valid resonant argument: the sum of all the integer coefficients ($p+q$, $-p$, and j_i) must be zero; and the sum of j_1 and j_2 must be an even number, or nodes must appear in pairs. When two satellites are out of resonance, ϕ circulates through a full 360° over time. But when they are in resonance, ϕ is constant, and Eq. (4) implies $(p+q)n_1 - pn_2 \approx 0$ since nodes and pericenters vary

much slower than mean longitudes. Although the two satellites are not exactly commensurate, they are still very close to. The integer q is the order of the resonance, which is relevant to the resonant strength. Higher order means weaker resonance. q determines how many nodal and pericenter parameters may appear in the resonant argument, while each of those parameters is corresponding to multiplying a e or $\sin i$ in the resonant strength. Since e's and $sini$'s are small quantities, the more they are, the weaker the resonance is.

The rates of all six parameter in Eq. (4) depend on the semimajor axes of the satellites. When satellites tidally migrate, their resonant state changes (see Greenberg et al. 1972; Greenberg 1973; Peale 1986; Hamilton and Burns 1993; Hamilton 1994; Murray and Dermott 1999). When the two orbits diverge from each other and pass through a resonance, the affected orbital elements are subject to sharp changes, which can be either positive or negative. The signs and magnitudes of these kicks depend on not only the resonant strength, but also the initial phase when the two step into the resonance. However, they are predictable if the two diverge very slowly so that the variation of orbital elements are in adiabatic limit before and after resonance encounter. In this case the kicks on eccentricities and inclinations are always positive, and the amounts of kicks can be obtained analytically by a Hamiltonian analysis (see Peale 1986; Murray and Dermott 1999). In contrast, when the two orbits pass through a resonance when they approach each other, the two can be captured into resonant state and remain in resonance unless perturbations from other objects or other nearby resonances force them out. During a resonance capture, the affected eccentricities and/or inclinations keep growing and the orbits may be forced to fairly eccentric and tilted.

In this paper we focus on the resonance encounters between Proteus and Larissa. Since they are on different side of the synchronous orbit and migrate away from each other, only resonant kicks can happen. However, we will see in a later section that, in cases when two nearby resonances overlap, it is possible that they can be temporarily captured into some resonances. The tidal migration rates of Proteus and Larissa are slow enough so that most of the first- and second-order resonances are in adiabatic limit. We cannot predict the amount of kicks from higher order resonances, but they are usually weaker by an order of magnitude. We are still able to estimate how much inclination the satellites can obtain through each resonance passage with fair precision. Based on Eq. (1), we calculate the possible first- and second- order resonances between the two in the past (Fig. 2). Because Eq. (1) is over-simplified in the vicinity of synchronous orbit, the left end of the plot is less accurate. In fact, it is very likely that Larissa formed well inside the synchronous orbit and moved much slower than predicted by Eq. (1) in early stages. The actual evolutionary timescale depends on Neptune's Q, which we will constrain through later discussions. We assumed a mass ratio of 0.1 between Larissa and Proteus based on the sizes given in Karkoschka (2003). As the resonant locations get closer with increasing p, a lot more resonances may fit in for a slightly different mass ratio. However, we will see that the strong interaction between first order eccentricity resonances for big p forces the orbital elements to behave chaotically and wipes out all previous resonance signatures.

4. Numerical Techniques

Our simulations are carried out with *HNDrag* in the *HNBody* package (Rauch and Hamilton 2005). *HNBody* is a general purpose hierarchical N-body integrator, which implements both symplectic and high order Burlisch-Stoer and Runge-Kutta algorithms. *HNDrag* expands the original *HNBody* codes, which enable us to add any artificial drag forces to the satellites, which can simulate a wide range of external perturbations. Since our interest lies in the long-term orbital evolution and we do not care about the location of the satellites in their orbits, we use the symplectic integrator for better time-wise performance. The integration stepsize is chosen so that there are at least 20 steps during each orbital period. In each simulation, the system consists of Neptune, Triton, Proteus and Larissa. We fix the semimajor axis of Larissa, and migrate Proteus outwards across each individual resonances. The drag force we use simply drive Proteus away from Neptune in a steady rate. In reality, the diverging speed or the two satellites might accelerate or decelerate. But since most of the strong resonances are in adiabatic limit, the kicks on the eccentricities and inclinations are independent of this acceleration as long as they diverge slow enough. We ignore the Sun in our simulations since the Solar tidal perturbation is much smaller than Triton's at Neptune vicinity.

The output of *HNDrag* can be either osculating orbital elements or Cartesian positions and velocities. The osculating elements are a set of projected Kepler orbital elements for each instant, assuming no extra perturbations. However, perturbations from both Neptune's oblateness and Triton exist, which cause the osculating elements of orbits to vary with orbital mean motions, resulting artificial oscillations in the outputs. We can get ride of this artificial effect by using geometric elements, which define the real shape of the orbit. Following (Greenberg 1981), we take the positions and velocities outputs from *HNDrag* and convert them to geometric orbital elements with a separate program called *cj2*. *cj2* only correct for perturbation from Neptune's oblateness, which by far contribute for most of the artificial oscillation. Small oscillations still show up in our plots of orbital elements due to other perturbations, but their magnitudes are too small to hide any interesting changes.

5. Resonances between Proteus and Larissa

As Proteus and Larissa tidally migrates to their current orbits, they have passed through a series of mean-motion resonances (c.f. Fig. 2). The satellites gain eccentricity and inclination through each resonant passage. Although the eccentricities obtained through earlier passages have damped away, the acquired inclinations are well preserved until today. In this section, we discuss our simulations for each of the individual resonances.

5.1. 5:3 Resonances

Although it is neither the earliest nor the latest of the series of resonant passages Proteus and Larissa have gone through, the 5:3 mean resonance is the simplest in that there are not any distracting first- and third-order resonances occurring in the same region. The next strongest resonances coinciding are of fourth-order (10:6), which are too weak to even show up on most of our plots.

5.1.1. Second-order Mean Motion Resonances without Triton

Before looking at the change of orbital elements in the real system, we examine the 5:3 resonances in an ordinary system with only two satellites, Fig. 6 shows the orbital semimajor axes, eccentricities, and inclinations of the two satellites when they diverge through their 5:3 mean motion resonance without Triton's presence. During the outwards migration of Proteus, the orbital elements of the two jumps at six locations, corresponding to three eccentricity-type and three inclination-type second-order resonances which are split out from the mean-motion resonance due to orbital precession. Both the two types of resonances are equally-spaced, which can be explained by looking through the resonant arguments. When the two satellites are in resonance, the resonant argument satisfies:

$$\dot{\phi} = 0. \tag{5}$$

For the three inclination resonances, which we name as $R_{i_P^2}$, $R_{i_P i_L}$, and $R_{i_L^2}$ from the left to the right in Fig. 6, the corresponding resonant arguments are:

$$\phi_{i_P^2} = 5\lambda_{P1} - 3\lambda_L - 2\Omega_{P1}, \tag{6}$$

$$\phi_{i_P i_L} = 5\lambda_{P2} - 3\lambda_L - \Omega_L - \Omega_{P2}, \tag{7}$$

$$\phi_{i_L^2} = 5\lambda_{P3} - 3\lambda_L - 2\Omega_L, \tag{8}$$

where the subscripts $1, 2, 3$ denotes the 3 different location of Proteus. Eq. (5) requires that,

$$5n_{P1} - 3n_L - 2\dot{\Omega}_{P1} = 0, \tag{9}$$

$$5n_{P2} - 3n_L - \dot{\Omega}_L - \dot{\Omega}_{P2} = 0, \tag{10}$$

$$5n_{P3} - 3n_L - 2\dot{\Omega}_L = 0. \tag{11}$$

Since the 3 resonance locations are very close, we can safely neglect the difference between the nodal precession rates. Eqs. (9-11) imply

$$n_{P1} - n_{P2} \approx n_{P2} - n_{P3}, \tag{12}$$

which, for close resonance locations, is equivalent to

$$a_{P2} - a_{P1} \approx a_{P3} - a_{P2}. \tag{13}$$

Furthermore, since the migration rate of Proteus is nearly constant over a short period of time, these locations are equally spaced in time as well(Fig. 6).

The resonance strength depends on the strength of perturbation and the instant values of the orbital elements. Since the mass of Proteus is much larger than that of Larissa, the perturbation on Larissa is much stronger than on Proteus. Hence the inclinations and eccentricities of Larissa changes much more than Proteus. The strengths of $R_{i_P^2}$, $R_{i_P i_L}$, and $R_{i_L^2}$ depend on i_P^2, $i_P i_L$, and i_L^2, respectively. Because $i_P > i_L$ in the simulation, the $R_{i_P^2}$ kick on i_P is stronger than the $R_{i_P i_L}$ kick, and the $R_{i_P i_L}$ kick on i_L is stronger than the $R_{i_L^2}$ kick. The detailed analysis of these resonances can be found in Murray and Dermott (1999).

5.1.2. Laplacian Plane and Free Inclination

When we add Triton into the system, this symmetric pattern changes. Although the eccentricity kicks are about the same, the inclination resonance pattern varies dramatically. But before we analyze the details of the new pattern, we find a problem with the resonant angle. Usually, when the two satellites pass through a resonance, the corresponding resonant argument has a stationary value at the exact resonant location. However, the resonant angles of the three second-order inclination-type resonances, as defined in Eqs. (6-8), keep circulating in full 360°. We figure out that the presence of Triton has revised the resonant arguments. We need to redefine some of the nodal elements to re-validate the definition of the resonant angles in the unique Neptune-Triton system.

In a two-body system consisting of Neptune and Triton, if Neptune were perfectly spherical, the two would have circulated around each other in Keplerian orbits. The rotational angular momentum of Neptune ($\mathbf{L}_N$) and the orbital angular momentum of Triton ($\mathbf{L}_T$) are both constants with fixed directions in space. In reality, however, the oblateness of Neptune resulting from spin deformation cause Triton's orbital plane to precess. To the second order in the ratio between the radius of Neptune (R_N) and the semimajor axis of Triton (a_T), the nodal precession rate is determined by (Danby 1988)

$$\dot{\Omega_T} = -n_T \frac{3}{2} J_2 \left(\frac{R_N}{a_T} \right)^2 \equiv g_T^{obl}, \tag{14}$$

where J_2 is a dimensionless constant which quantifies the planet's oblateness. For Neptune and Triton, $J_2 = 0.003411$, and $\dot{\Omega_T}$ is about 600 years which is sufficiently longer than Triton's orbital period (5.88 days).

Although $\mathbf{L}_T$ is no longer a constant vector due to the precession of Triton's orbital plane, the system still conserves its total angular momentum $\mathbf{L}_{tot} = \mathbf{L}_N + \mathbf{L}_T$, and the plane perpendicular to $\mathbf{L}_{tot}$ is fixed in space, which makes it a natural reference plane for orbital elements measurement. This plane is usually referred as the invariable plane. In the Neptune-Triton system, it is tilted $\epsilon = 0.5064°$ from Neptune's equatorial plane (Jacobson and Owen 2004). Neptune's equatorial

plane is always locked with Triton's orbital plane, and the two precess together along the invariable plane. Here we ignore the spin of Triton and orbits of the other satellites since their contributions are negligible.

Small inner Neptunian satellites ($m \ll m_T \ll m_N$) experience not only perturbation from Neptune, which cause their orbits to precess with a rate g^{obl} similar to g_T^{obl} in Eq. (14), but also secular perturbation from Triton. To second order in small eccentricities and inclinations, the semimajor axes of small satellites do not change and the equations governing the changes of eccentricities and pericenters are completely separable from those determining how inclinations and nodes vary. Because Triton's eccentricity is close to zero, it has minimal effect on the eccentricities and pericenters of small moons. But the inclinations of those moons are perturbed a lot due to Triton's large tilt.

Murray and Dermott (1999) show that an external perturber, Triton, causes the node of a small inner satellite to precess with frequency

$$g^{sec} = -\frac{1}{4} n \frac{m_T}{m_N} \alpha^2 b_{3/2}^{(1)}(\alpha). \tag{15}$$

Here $\alpha = \frac{a}{a_T}$ is the semimajor axes ratio of the satellite and Triton, and $b_{3/2}^{(1)}(\alpha)$ is one of the Laplace coefficients. Combined with the perturbations from Neptune's oblateness, the disturbing function for the small satellite can be written as

$$\mathcal{R} = na^2 \left\{ \frac{1}{2}(g^{sec} + g^{obl}) i^2 - g^{sec}(\pi - i_T) i \cos(\Omega - \Omega_T - \pi) \right\}, \tag{16}$$

where the extra π symbols are due to Triton's retrograde orbit. We solve the Lagrange's planetary equation with the above disturbing function, and get

$$i \sin\Omega = i^{fr} \sin[(g^{sec} + g^{obl})t + \delta\,] + i^{Lap} \sin(\Omega^{Lap}), \tag{17}$$

$$i \cos\Omega = i^{fr} \cos[(g^{sec} + g^{obl})t + \delta\,] + i^{Lap} \cos(\Omega^{Lap}), \tag{18}$$

where the free inclination i^{fr} and phase angle δ are constants determined by initial states. The angles i^{Lap} and Ω^{Lap} define the local Laplacian plane of the satellite as illustrated in Fig. 3a.

$$i^{Lap} = \frac{g^{sec}}{g^{sec} + g^{obl}}\ (\pi - i_T), \tag{19}$$

and

$$\Omega^{Lap} = \Omega_T + \pi, \tag{20}$$

both of which are independent of the initial inclination and node of the satellite. Once the satellite's semimajor axis is given, its local Laplacian plane is determined, which precess together with Triton's orbit and Neptune's equator. i^{Lap} and Ω^{Lap} are usually called forced inclination and node.

Fig. 3b illustrates the solutions (17-18) in a phase diagram of $i \sin\Omega$ versus $i \cos\Omega$. The magnitudes of vectors $\overrightarrow{OO'}$ and $\overrightarrow{O'A}$ are the forced and free inclinations, respectively. The direction

of $\overrightarrow{OO'}$ gives the forced node Ω^{Lap}, and the direction of $\overrightarrow{O'A}$ measured from $\overrightarrow{OO'}$ is Ω^{fr}. The vector sum of the two represents the inclination i and longitude of ascending node Ω of the small satellite relative to the invariable plane and an arbitrary reference direction. Measuring the direction of $\overrightarrow{O'A}$ from the reference direction, we get the angle

$$\tilde{\Omega} = \Omega^{Lap} + \Omega^{fr}, \tag{21}$$

which we redefine as the longitude of ascending node of the satellite. Fig. 3a shows its physical meaning: a bent angle occupying two different plane which is similar to the definition of the longitude of pericenter ϖ.

The free inclination can be looked on as inclination of the satellite measured from its local Laplacian plane, and the free node is measured from the node of the Laplacian plane. Fig. 4 shows the difference between i,Ω and i^{fr}, Ω^{fr}. Measured relative to the Laplacian plane, i^{fr} is a constant over time and Ω^{fr} regress constantly. However, measured relative to the invariable plane, i oscillates around i^{Lap} and Ω, in addition to regress, progresses at the same rate as the Laplacian plane. Besides regress along the Laplacian plane, the orbit of the satellite has be forced to progress with it as well.

Another way of thinking about satellite's local Laplacian plane is that, suppose we are putting satellites into the Neptune-Triton system. If a satellite starts right in its local Laplacian plane, or its initial inclination is i^{Lap}, it always stay in the plane and its inclination stays constant relative to any reference plane. However, if it starts out of its local Laplacian plane, i.e. with a non-zero free inclination, it precesses along the plane and its inclination measured from any other plane oscillates.

Since i^{Lap} depends on the semimajor axis of a satellite, satellites at different distances from Neptune will have different local Laplacian plane. When Triton is circularized and forced the original satellites of Neptune in to debris, those debris damps into their local Laplacian plane very quickly (in the order of several years Banfield and Murray 1992). The disk is very thin, similar to Saturn's rings, and is warped along the Laplacian plane as shown in Fig. 5. The whole warped disk precesses as a unit along with Triton's orbit and Neptune's equator.

With the new defination of the longitude of the ascending node $\tilde{\Omega}$, resonant arguments defines in Eqs. () hold in the Neptune-Triton system. The resonances kick free inclinations up or down instead of the inclinations relative to invariable plane. The resonance strengths also directly depend on free inclinations.

5.1.3. Three-body Resonances

Now we look into details of the 5:3 resonance passage of Proteus and Larissa with Triton in the system. Fig. 7 shows the free inclinations of Larissa and Proteus. In addition to the 3 second-order resonance kicks, two strong kicks, $R_{i_L i_T}$ and $R_{i_P i_T}$ show up. The space between $R_{i_L i_T}$ and $R_{i_P i_L}$ is

the same as that between $R_{i_P i_T}$ and $R_{i_P^2}$. Because the resonance arguments of $R_{i_P i_L}$ and $R_{i_P^2}$ are

$$\begin{aligned} \phi_{i_P i_L} &= 5\lambda_P - 3\lambda_L - \tilde{\Omega}_P - \tilde{\Omega}_L, \\ \phi_{i_P^2} &= 5\lambda_P - 3\lambda_L - 2\tilde{\Omega}_P, \end{aligned} \tag{22}$$

and because $R_{i_L i_T}$ only affects Larissa and $R_{i_P i_T}$ only affects Proteus, we assume that the resonance arguments for them are somehow similar to

$$\begin{aligned} \phi_{i_L i_T} &= 5\lambda_P - 3\lambda_L - \tilde{\Omega}_L, \\ \phi_{i_P i_T} &= 5\lambda_P - 3\lambda_L - \tilde{\Omega}_P. \end{aligned} \tag{23}$$

However, there are two problems with these arguments. First, the sum of the coefficients of either is not zero; second, the nodes do not appear in pairs. We need another node parameter in either of the resonance arguments. The missing part turns out to be the node of the satellites' local Laplacian plane, and the resonances can be interpreted as resonances between the satellites and their local Laplacian planes, which always precess with Triton. The real resonance arguments write as

$$\begin{aligned} \phi_{i_L i_T} &= 5\lambda_P - 3\lambda_L - \tilde{\Omega}_L - \Omega^{Lap}, \\ \phi_{i_P i_T} &= 5\lambda_P - 3\lambda_L - \tilde{\Omega}_P - \Omega^{Lap}. \end{aligned} \tag{24}$$

Since the precession of Laplacian plane is much slower than that of the orbits of the satellites, the adding terms do not shift the resonance location much. Fig. 7 also shows the 2 corresponding resonant arguments. When the two satellites are close to R_{i_L} and R_{i_P}, the corresponding ϕ_{i_L} or ϕ_{i_P} do not circulating whole 360° any longer. Instead, they begin to oscillate around some certain values, i.e. 180° for Larissa and 0° for Proteus. Physically, when the two satellites are far away from resonance, their orbits precess along their local Laplacian planes all around due to Neptune's oblateness and secular perturbations among the satellites, and their orbital planes shifts up and down crossing them. When they migrate close to the resonance, the orbit of the affected satellite turns around and starts to regress relative to the node of the Laplacian plane at some point. After regressing through the equilibrium point and to the other end of the libration, it turns around and begins to precess again. The libration magnitude decreases as the two satellites getting closer to the resonance location, at which point the orbit of the affected satellite is completely locked up with the Laplacian plane, and precess together with Triton until tides bring them out of resonance. Once leaving resonance, the orbits begin to circulate again.

Since local Laplacian plane is only a mathematical way of describing the orbital system, these new resonances are better interpreted as 3-body resonances among Larissa, Proteus, and Triton. However, it is different from all other 3-body resonances that have been studied (e.g. Laplace resonance among Jupiter's satellites: Io, Europa, and Ganymede) in that Triton's longitude does not appear in the resonance arguments. However, Triton's node is involved in both arguments (since $\Omega^{Lap} = \Omega_T + \pi$), which implies its inclination should be kicked at resonance. In reality, because Triton is much more massive than Proteus and Larissa, it is hardly perturbed by them.

For the 3 2-body resonances, the corresponding inclination kicks are weaker compared to the previous case in which Triton is not included. In both of the simulations, the initial inclinations of both satellites relative to Neptune's equator are the same, which are the tilts of the satellites' local Laplacian plane. However, for the later case, the resonance strength depends directly on the free inclinations relative to the local Laplacian planes, which are tiny. Hence the kicks are not as strong.

Although the 2-body resonances are weak for small free inclinations, Proteus and Larissa are still able to gain inclinations because the 2 new strong 3-body resonances. To measure the amount of inclination kicks through the 5:3 passage, we need to make sure that Proteus migrates slowly enough in our simulation so that the system is in adiabatic limit. We have done a series of simulations with the same initial configuration but different Proteus migration rate and measured the amount of jumps resulting from the 6 major resonance kicks. The results are shown in Fig. 8. The plots imply that if Proteus migrates at a rate $5 \times 10^{-13} R_N/day$ or slower, the 2 3-body kicks are in adiabatic limit, the $R_{i_P i_L}$ kicks and $R_{i_L^2}$ kick are near the limit, while the $R_{i_P^2}$ kick on Proteus may be quite away from the limit. However, the later is much weaker that others, and it only has small effect on the final inclination of Proteus. The slowest migration rate we used in our simulations is $5 \times 10^{-13} R_N/day$, at which Proteus migrates about one Neptune radius over the age of the system. Measured from Fig. 7, Proteus obtains a free inclination of 0.012° and Larissa's tilt is kicked up by 0.068°, both of which are less than half of their current free tilts.

Apparently, a single mean-motion passage is not powerful enough to kick the inclinations of Proteus and Larissa to their current values, even with the strong 3-body resonances. However, since inclination damps very slow and resonances in adiabatic limits always kick inclinations up, multiple passages can do the job. Before we look through other recent mean motion resonances between Proteus and Larissa, we need to determine how the kicks from different resonances add up. Studies (references?) show that for 2-body resonances, a larger initial tilt always results a greater kick. However, for the three-body resonance, the amount of kick scale with the initial free inclination in a different way. Fig. 9 shows how the $R_{i_L i_T}$ kick magnitude changes with different initial i_L's. In contrast to the two-body case, the kick magnitude decreases with increasing initial free inclination. For large i_{L0}, Δi_L scales as

$$\Delta i_L \propto i_{L0}^{-\frac{1}{2}}.$$

In two-body resonances, the resonance kick scales up with initial inclination because the resonance strength increases with inclination, and absolute inclinations relative to the equator of Neptune do not effect the relative distance of the two satellites much, although their mutual inclination matters. In 3-body case, large free inclination also means the small satellites are further away from Triton, which results a decrease in the resonance strength.

5.2. 2:1 Resonances

The most recent resonance encounter between Proteus and Larissa is their 2:1 resonance, which is only about $600km$ outside Larissa's orbit or $900km$ inside Proteus's orbit. Their excited eccentricities have yet been tidally damped away (Table 1). Unlike the 5:3 resonance, in which the next higher-order resonances is fourth-order (10:6), the 2:1 resonance coincides with resonances of any single order, i.e., 4:2 (second-order), 6:3 (third-order), 8:4 (fourth-order) etc. With all those different order resonances on top of each other, the changes of orbital elements during the pass of this resonance, shown in Fig. 10, is very complicated. The eccentricity resonances include two strong first-order ones and a bunch of much weaker higher-order ones, among which the second-order $R_{e_L e_P}$ is the strongest, but the magnitudes of kicks are still tiny. The inclination resonances are much more complicated than those in the 5:3 case. The two second-order three-body resonances are still the strongest among all the inclination jumps. Couple of new fairly strong third-order three-body resonances show up, which contribute a significant amount towards the total inclination gains.

5.2.1. Eccentricity Resonances and Q's of the Satellites

The current eccentricities of Larissa and Proteus are 0.002046 and 0.000258, respectively, which have been tidally damping away over the last hundred million years after they are excited through the 2:1 mean motion resonance of the two satellites. Since tidal migration is determined by planetary tides (Eq. 1) and eccentricity damping is mostly accounted by satellite tides (Eq. 2), the ratio between satellite Q and Q_N can be estimated based on satellite's migration distance and the change of its eccentricity :

$$\frac{Q}{Q_N} = \frac{21}{4}\frac{k_{2N}}{\tilde{\mu}}\left(\frac{m_N}{m}\right)^2\left(\frac{R}{R_N}\right)^5\left|\frac{d\,\ln a}{d\,\ln e}\right|. \tag{25}$$

For the tidal migration after the 2:1 resonances, we know that the initial values of semimajor axes must satisfy $a_P/a_L = 2^{\frac{2}{3}}$, they evolve following Eq. (1), and the two satellites migrate to their current orbits at the same time. We calculated the changes of the semimajor axes of the two satellites based on these constraints: Larissa has migrated $0.016R_N$ towards Neptune, while Proteus has moved $0.011R_N$ outward. We obtained the initial eccentricities of the two satellites right after their resonance by numerical simulations. Since the eccentricity resonances are first-order, they are much stronger and our simulations show that the two strong eccentricity kicks in Fig. 10 are well within the adiabatic limit. The higher-order kicks are too weak to have any significant effect. Hence eccentricities measured after the kicks, which are 0.011 for Larissa and 0.0016 for Proteus, are close to their actual values when they left the resonant configuration.

With these measures of change of a's and e's, the Q of Larissa and Proteus can be computed with respect to Q_N:

$$Q_L = 0.029\,Q_N,\ Q_P = 0.014\,Q_N. \tag{26}$$

5.2.2. Inclination Resonances

5.3. 3:2 Resonances

6. Discussion

Constraints on Neptune's Q and the formation location of Larissa and Proteus by which resonances have to or must not happen. Constraints on Q's of Larissa and Proteus.

Further work: High inclination of Naiad; Ring arc shepherds.

REFERENCES

Agnor, C. B., Hamilton, D. P., 2005. Satellite capture via binary exchange reactions: application to Triton. AAS/Division of Dynamical Astronomy Meeting 36, 11.05.

Banfield, D., Murray, N., 1992. A dynamical history of the inner Neptunian satellites. Icarus 99, 390–401.

Burns, J. A., 1977. Orbital evolution. In: Burns, J. A. (Ed.), Planetary Satellites. Univ. of Arizona Press, Tuscon, AZ, USA, pp. 113–156.

Danby, J. M. A., 1988. *Fundamentals of Celestial Mechanics*. Willmann-Bell Inc., 2nd rev. & enlarged ed., Richmond, VA, USA.

Darwin, G. H., 1880. On the secular effects of tidal friction. Astronomische Nachrichten 96, 217–222.

Goldreich, P., Murray, N., Longaretti, P. Y., Banfield, D., 1989. Neptune's story. Science 245, 500–504.

Goldreich, P., Soter, S., 1966. Q in the Solar System. Icarus 5, 375–389.

Goldreich, R., 1963. On the eccentricity of satellite orbits in the solar system. MNRAS 126, 257–268.

Greenberg, R., 1973. Evolution of satellite resonances by tidal dissipation. AJ 78, 338–346.

Greenberg, R., 1977. Orbit-orbit resonances among natural satellites. In: IAU Colloq. 28: Planetary Satellites. pp. 157–167.

Greenberg, R., 1981. Apsidal precession of orbits about an oblate planet. AJ 86, 912–914.

Greenberg, R. J., Counselman, C. C., Shapiro, I. I., 1972. Orbit-orbit resonance capture in the Solar System. Science 178, 747–749.

Hamilton, D. P., 1994. A comparison of Lorentz, planetary gravitational, and satellite gravitational resonances. Icarus 109, 221–240.

Hamilton, D. P., Burns, J. A., 1993. Lorentz and gravitational resonances on circumplanetary particles. Adv. Space Res. 13 (10), 241–248.

Hamilton, D. P., Zhang, K., Agnor, C., 2005. Constraints on Triton's orbital evolution. AAS/Division of Dynamical Astronomy Meeting 36, 11.04.

Jacobson, R. A., Owen, W. M., 2004. The orbits of the inner Neptunian satellites from Voyager, Earth-based, and Hubble Space Telescope observations. AJ 128, 1412–1417.

Jeffreys, H., 1961. The effect of tidal friction on eccentricity and inclination. MNRAS 122, 339–343.

Karkoschka, E., 2003. Sizes, shapes, and albedos of the inner satellites of Neptune. Icarus 162, 400–407.

McKinnon, W. B., 1984. On the origin of Triton and Pluto. Nature 311, 355–358.

Murray, C. D., Dermott, S. F., 1999. *Solar System Dynamics*. Cambridge University Press, Cambridge CB2 2RU, UK.

Owen, W. M., Vaughan, R. M., Synnott, S. P., 1991. Orbits of the six new satellites of Neptune. AJ 101, 1511–1515.

Peale, S. J., 1976. Orbital resonances in the Solar System. ARA&A 14, 215–246.

Peale, S. J., 1986. Orbital resonances, unusual configurations and exotic rotation states among planetary satellites. In: IAU Colloq. 77: Satellites. pp. 159–223.

Rauch, K., Hamilton, D. P., 2005. HNBody: A Symplectic Integration Package for Nearly-Keplerian Systems. in preparation.

Smith, B. A., Soderblom, L. A., Banfield, D., Barnet, C., Basilevsky, A. T., Beebe, R. F., Bollinger, K., Boyce, J. M., Brahic, A., Briggs, G. A., Brown, R. H., Chyba, C., Collins, S. A., Colvin, T., Cook, A. F., Crisp, D., Croft, S. K., Cruikshank, D., Cuzzi, J. N., Danielson, G. E., Davies, M. E., De Jong, E., Dones, L., Godfrey, D., Goguen, J., Grenier, I., Haemmerle, V. R., H., H., Hansen, C. J., Helfenstein, C. P., Howell, C., Hunt, G. E., Ingersoll, A. P., Johnson, T. V., Kargel, J., Kirk, R., Kuehn, D. I., Limaye, S., Masursky, H., McEwen, A., Morrison, D., Owen, T., Owen, W., Pollack, J. B., Porco, C. C., Rages, K., Rogers, P., Rudy, D., Sagan, C., Schwartz, J., Shoemaker, E. M., Showalter, M., Sicardy, B., Simonelli, D., Spencer, J., Sromovsky, L. A., Stoker, C., Strom, R. G., Suomi, V. E., Synott, S. P., Terrile, R. J., Thomas, P., Thompson, W. R., Verbiscer, A., Veverka, J., 1989. Voyager 2 at Neptune - Imaging science results. Science 246, 1422–1449.

Yoder, C. F., Peale, S. J., 1981. The tides of Io. Icarus 47, 1–35.

Table 1: Inner Neptunian satellites

Name	$\bar{R}$ (km)	e $(\times 10^{-3})$	i^{Lap} $(^\circ)$	i^{fr} $(^\circ)$
Naiad	33	$.362 \pm .301$	0.5118	4.7455 ± 0.0317
Thalassa	41	$.215 \pm .231$	0.5130	0.2094 ± 0.0212
Despina	75	$.224 \pm .176$	0.5149	0.0636 ± 0.0144
Galatea	88	$.037 \pm .090$	0.5262	0.0615 ± 0.0113
Larissa	97	$1.393 \pm .079$	0.5545	0.2046 ± 0.0088
Proteus	210	$.531 \pm .086$	1.0546	0.0258 ± 0.0069

References. — Sizes of the small satellites are from Karkoschka (2003); Orbital elements are from Jacobson and Owen (2004).

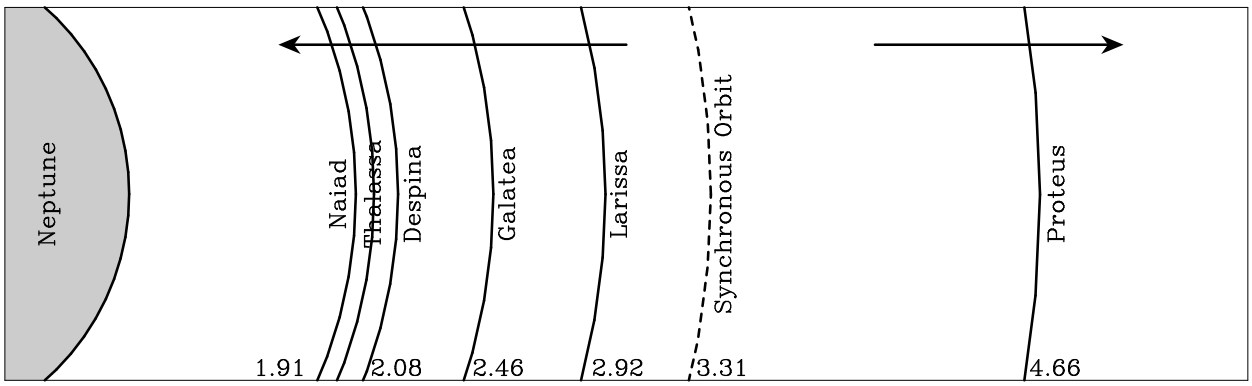

Fig. 1.— Semimajor axes of the small inner Neptunian satellites in R_N. The two arrows show the tidal migrating direction of the satellites. The dashed line indicates the synchronous orbit of Neptune.

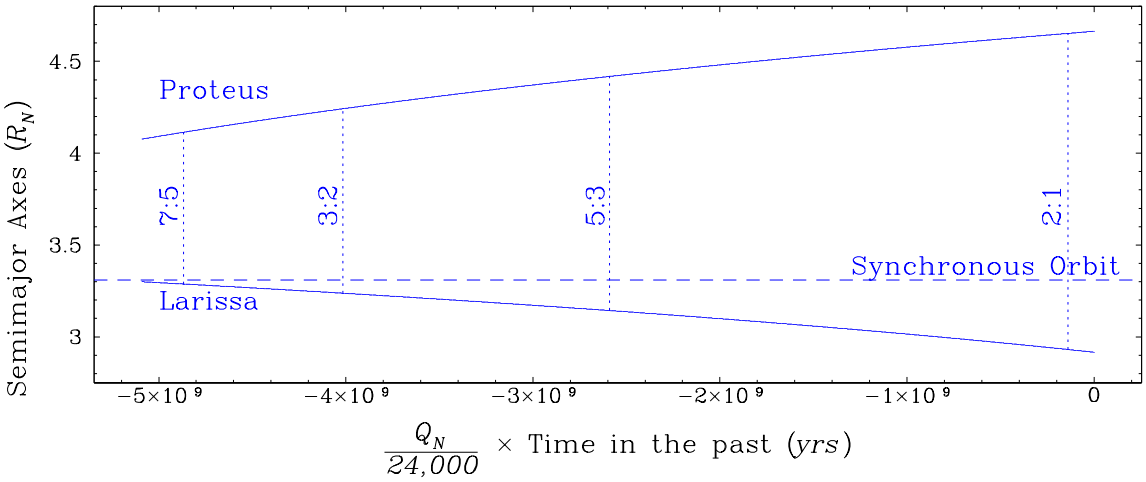

Fig. 2.— Possible past first- and second-order mean motion resonances between Proteus and Larissa. We integrate Eq. (1) backwards until Larissa reaches the synchronous orbit, which denotes the upper bound of its formation location. The mass ratio of Larissa and Proteus, estimated based on their size, is 0.1 in the calculation. The vertical dotted lines indicate locations of resonances.

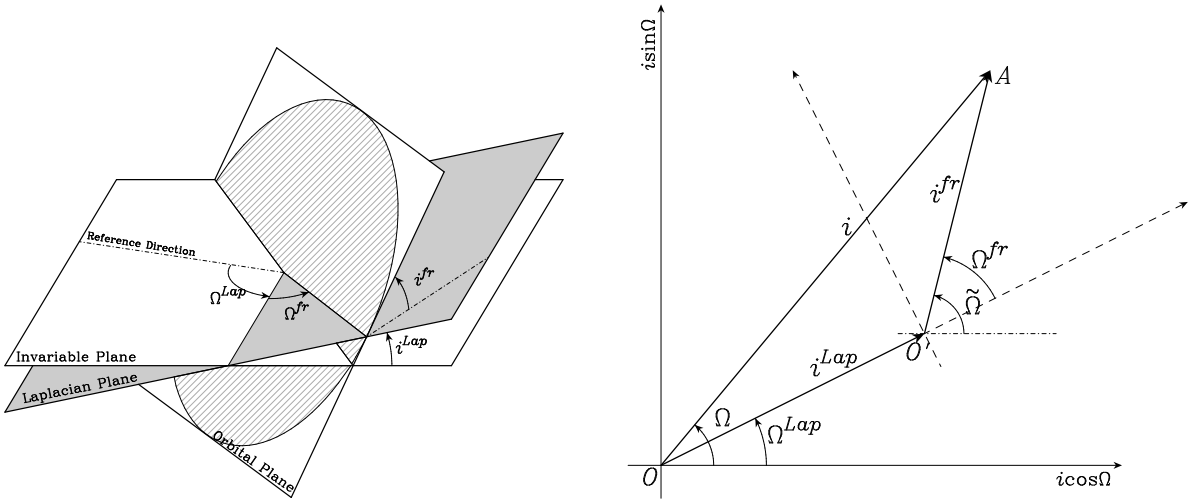

Fig. 3.— Definition of free orbital elements of a small satellite. i^{Lap}, Ω^{Lap}: inclination and longitude of ascending node of the local Laplacian plane; i^{fr}, Ω^{fr}: free inclination and node of the satellite's orbit measured relative to its local Laplacian plane; i, Ω: inclination and node of the satellite's orbit measured relative the invariable plane. The longitude of ascending node of the orbit is defined as the bend angle $\tilde{\Omega} = \Omega^{Lap} + \Omega^{fr}$. **a**: the physical representation of the planes and elements. **b**: phase diagram showing the solutions (17-18).

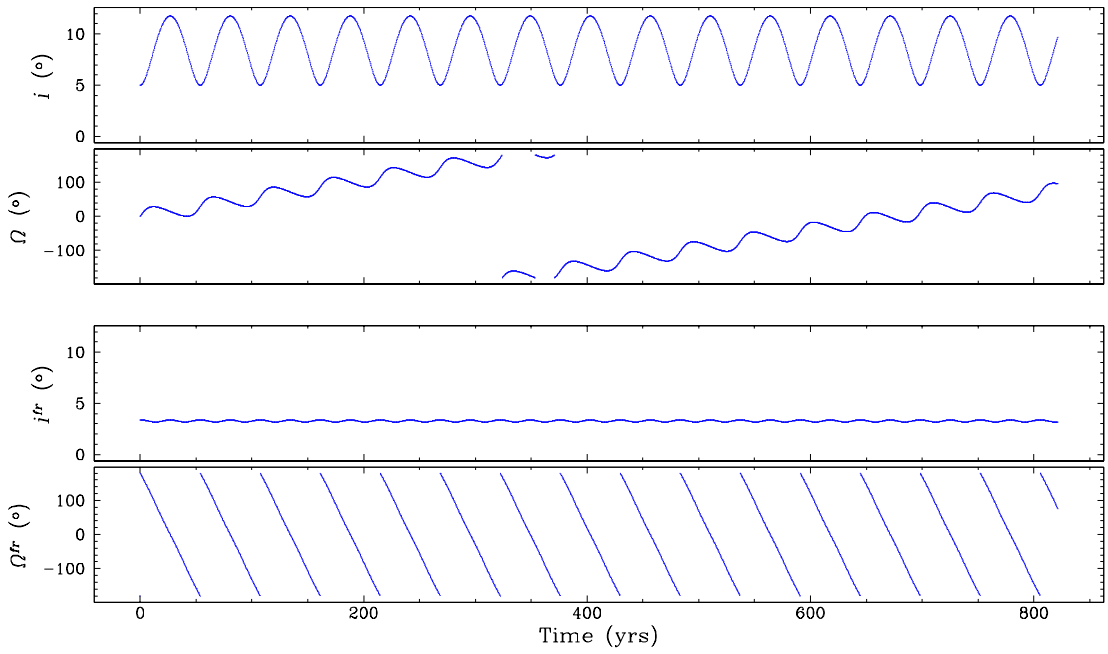

Fig. 4.— Inclination and node of a satellite at $a = 8R_N$ measured relative to the invariable plane (i, Ω) and the local Laplacian plane (i^{fr}, Ω^{fr}).

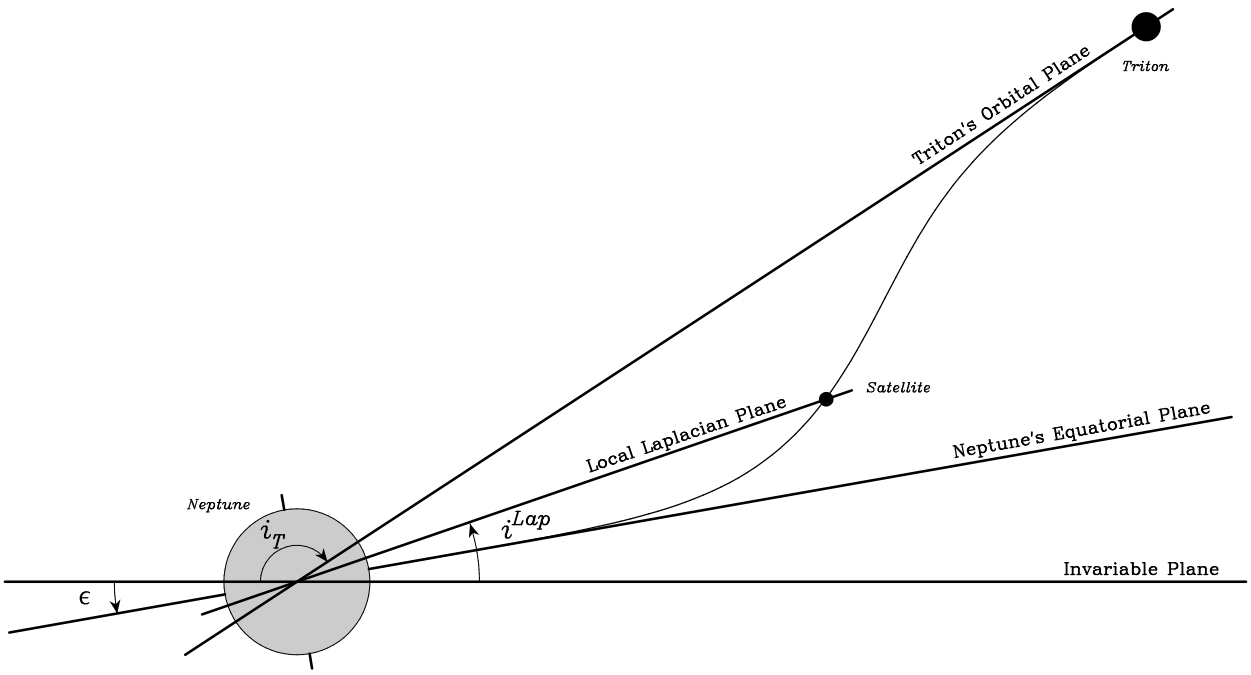

Fig. 5.— Laplacian plane of Neptune-Triton system. Plot shows a side view of the invariable plane, Neptunian equatorial plane, Triton's orbital plane, and the local Laplacian plane of a small satellite. i_T and ϵ are the inclinations of Triton's orbit and Neptune's equator, respectively. Note that they are measured towards different sides of the invariable plane due to the fact that Triton's orbit is retrograde. i^{Lap} is the inclination of its local Laplacian plane. The thin curve defines the shape of the warped Laplacian plane for a set of satellites with different semimajor axes, or a debris disk inside Triton's orbit. The whole Laplacian plane precess with Triton's orbit and Neptune's equator along the invariable plane.

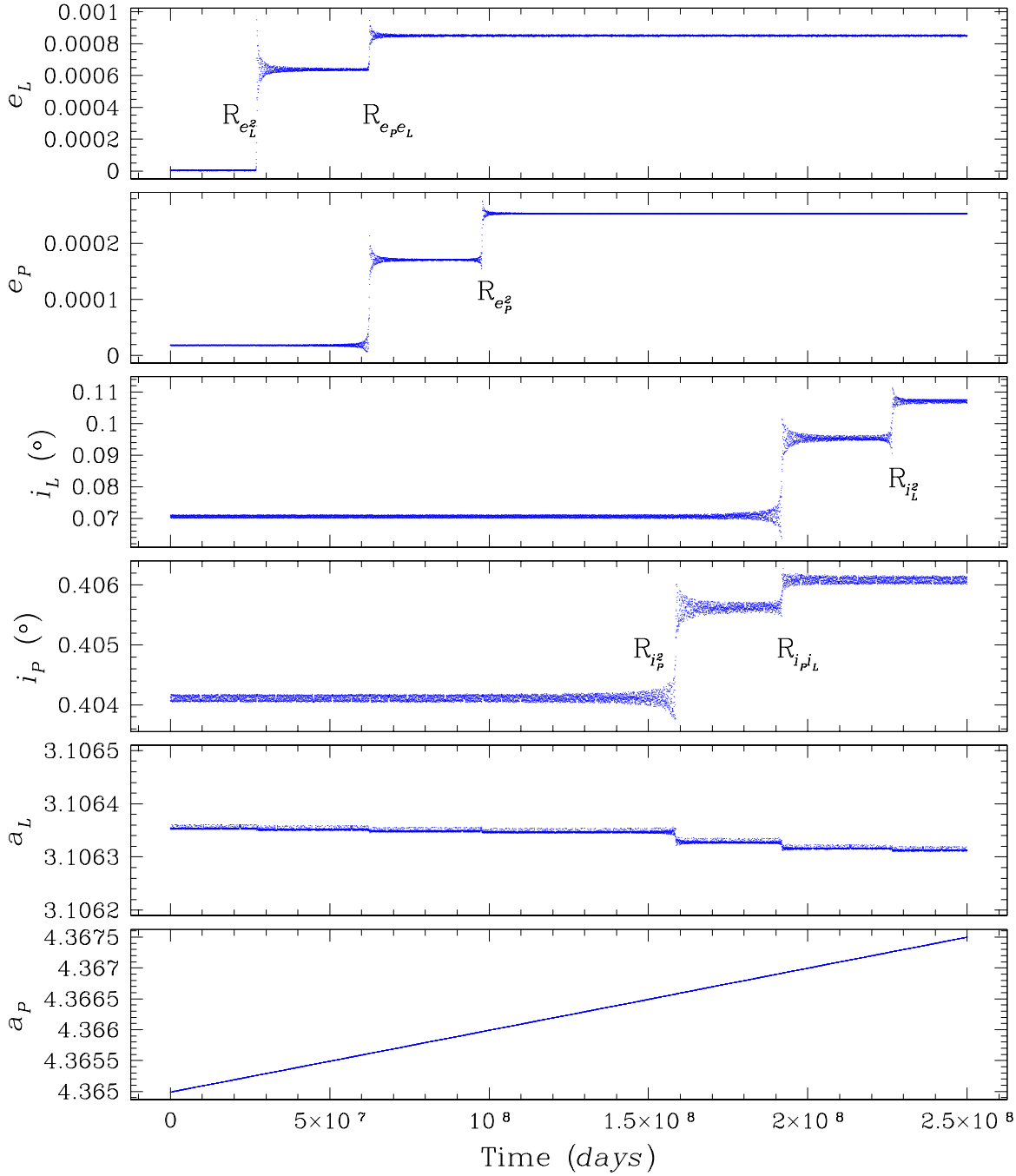

Fig. 6.— Proteus and Larissa diverge through their 5:3 mean motion resonance; Triton is excluded from the system. These plots show a typical second order mean motion resonance passage.

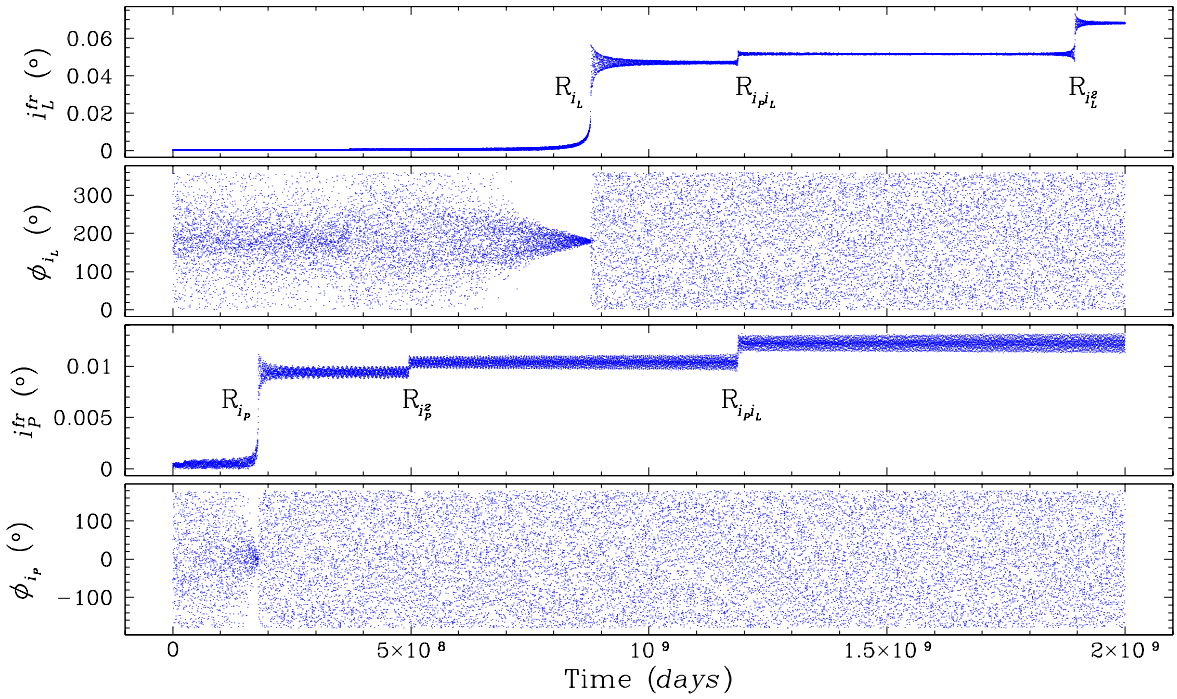

Fig. 7.— Proteus and Larissa diverge through their 5:3 mean motion resonance.

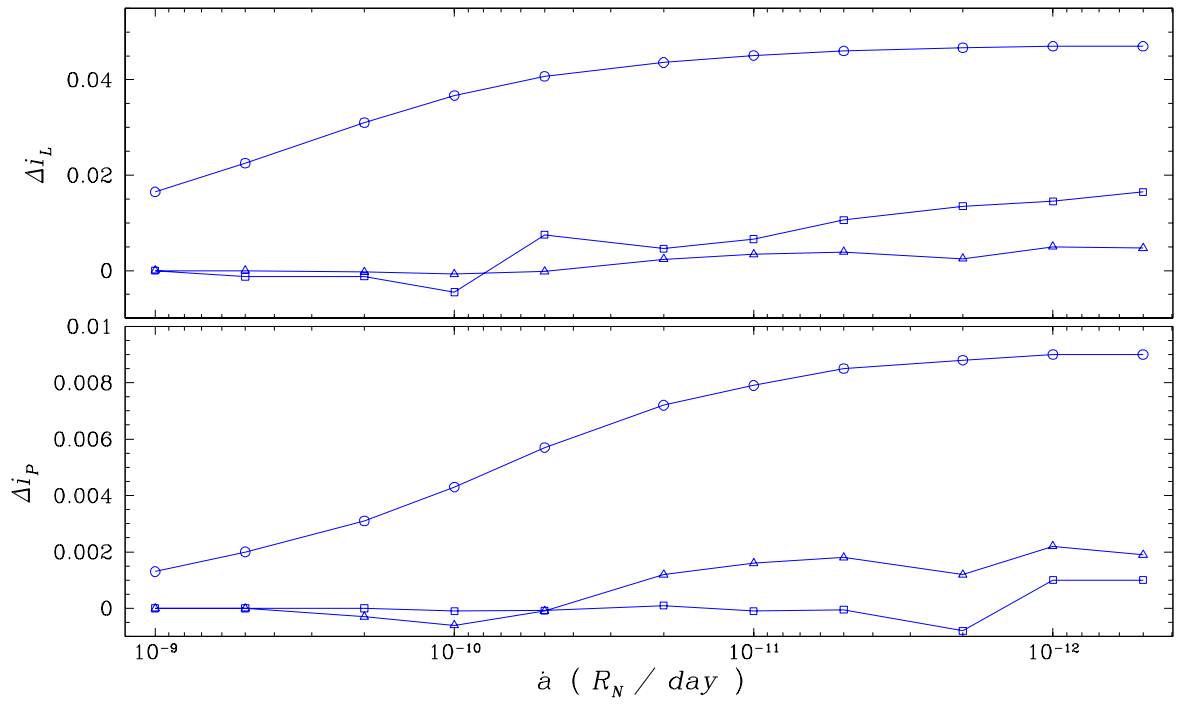

Fig. 8.— The kicks of inclinations of Proteus and Larissa from the 5 major resonances versus Proteus's migration rate when it diverges through their 5:3 resonances. Top: kicks of Larissa. *circle*: R_{i_L}; *triangle*: $R_{i_P i_L}$; *square*: $R_{i_L^2}$. Bottom: kicks of Proteus. *circle*: R_{i_P}; *triangle*: $R_{i_P i_L}$; *square*: $R_{i_P^2}$.

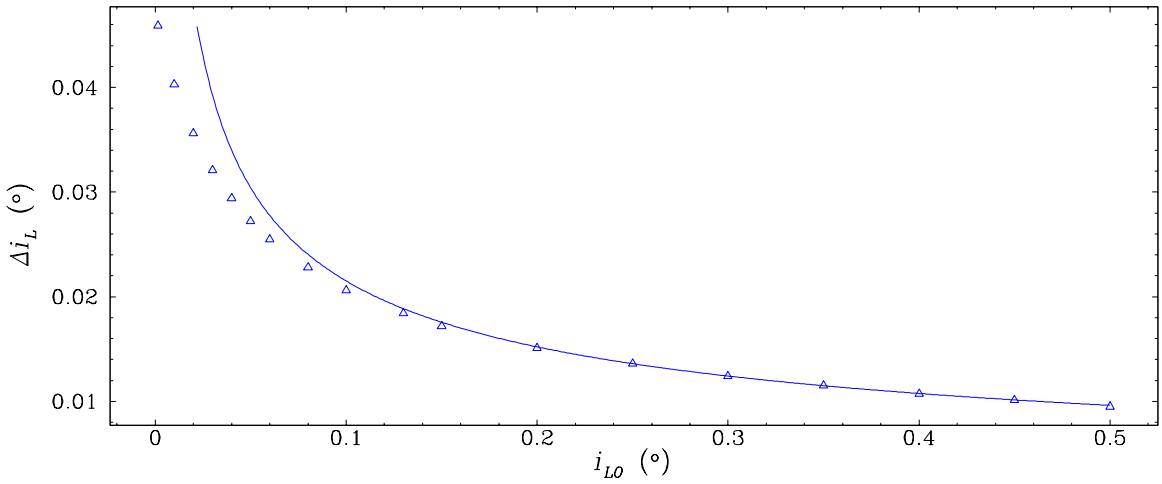

Fig. 9.— Magnitude of R_{i_L} kick on Larissa (Δi_L) versus its pre-kicked free inclination (i_{L0}). *Triangle*: kick magnitudes from different simulations with various initial free inclination of Larissa; *solid line*: fitted curve in which $\Delta i_L \propto i_{L0}^{-\frac{1}{2}}$.

Fig. 10.— Proteus and Larissa diverge through their 2:1 mean motion resonance.